

NONLINEAR BUCKLING ANALYSIS OF HYPERBOLIC COOLING TOWER SHELL WITH RING-STIFFENERS*

Li Long-yuan (李龙元) Loo Wen-da (卢文达)
(Shanghai Institute of Appl. Math. and Mech., Shanghai)

(Received Dec. 12, 1987)

Abstract

This paper is concerned with a numerical solution of hyperbolic cooling tower shell, a class of full nonlinear problems in solid mechanics of considerable interest in engineering applications. In this analysis, the post-buckling analysis of cooling tower shell with discrete fixed support and under the action of wind loads and dead load is studied. The influences of ring-stiffener on instability load are also discussed. In addition, a new solution procedure for nonlinear problems which is the combination of load increment iteration with modified R-C arc-length method is suggested. Finally, some conclusions having important significance for practice engineering are given.

I. Introduction

Hyperbolic shells are mostly used as natural draught cooling tower in the power plant and are made, as a rule, of reinforced concrete. With increasing capacity of the power plants it was necessary to increase both the height and the diameter of cooling tower shell. However, for such a large hyperbolic revolutionary shell under axisymmetric dead load and unaxisymmetric wind action, their stability problems received relatively less attention.

In recent years, due to the birth of high-speed computers, the rather accurate calculations have been developed for determination of the critical load, e.g., references [1-4,6,7] calculated the critical loads of cooling tower shells with various dimensions and boundary conditions for several loading cases. Ref. [5] gave the results of buckling tests in wind tunnel.

This paper is concerned with a numerical solution of hyperbolic cooling tower shell, a class of full nonlinear problems in solid mechanics of considerable interest in engineering applications. In this analysis, the post-buckling analysis of cooling tower shell with discrete fixed support and under the action of wind loads is studied. The influences of ring-stiffener on instability loads are also discussed. In addition, a new solution procedure for nonlinear problems which is the combination of load increment iteration with modified R-C arc-length method is suggested. Finally, some conclusions having important significance for practice engineering are given.

II. The Constitutive Equation of Reinforced Concrete with Inhomogeneous Reinforcement

In many structures of reinforced concrete, although both steel and concrete may be

* The Project Supported by National Natural Science Foundation of China.

homogeneous and isotropic, the reinforced concrete, as a composite material, is inhomogeneous and anisotropic owing to inhomogeneous reinforcement. Since the reinforcement is always designed as orthotropic in many practical structures, reinforced concrete is regarded as an inhomogeneous orthotropic structure.

Let ratios of reinforcement be ρ_x and ρ_y in the direction x and y . The elastic modulus and Poisson's ratio of steel are E_s and ν_s . Then, the relationship of stresses and strains in steel material may be written as

$$\begin{bmatrix} \sigma_x \\ \sigma_y \\ \tau_{xy} \end{bmatrix} = \frac{E_s}{1-\nu_s^2} \begin{bmatrix} 1 & \nu_s & 0 \\ \text{Symmetric} & 1 & 0 \\ & & (1-\nu_s)/2 \end{bmatrix} \begin{bmatrix} \varepsilon_x \\ \varepsilon_y \\ \gamma_{xy} \end{bmatrix} \quad (2.1)$$

The membrane forces per-unit length owing to strain $\{\varepsilon_x, \varepsilon_y, \gamma_{xy}\}$ are expressed in the following formulas

$$\{N_x^s, N_{yx}^s\} = \rho_x h \{\sigma_x, \tau_{yx}\}, \quad \{N_y^s, N_{xy}^s\} = \rho_y h \{\sigma_y, \tau_{xy}\} \quad (2.2)$$

It can be seen from equation (2.2) that $N_{xy}^s \neq N_{yx}^s$ if $\rho_x \neq \rho_y$.

Let

$$\bar{N}_{xy}^s = (N_{xy}^s + N_{yx}^s)/2$$

The corresponding relation of forces and strains can be expressed as follows

$$[N_s] = [D_s][\varepsilon_s] \quad (2.3)$$

where

$$[N_s] = \{N_x^s, N_y^s, \bar{N}_{xy}^s\}^T, \quad [\varepsilon_s] = \{\varepsilon_x, \varepsilon_y, \gamma_{xy}\}^T, \quad [D_s] = \frac{E_s h}{1-\nu_s^2} \begin{bmatrix} \rho_x & \nu_s \rho_x & 0 \\ \nu_s \rho_y & \rho_y & 0 \\ 0 & 0 & \rho_{xy}(1-\nu_s)/2 \end{bmatrix},$$

$$\rho_{xy} = (\rho_x + \rho_y)/2$$

In the same way, the relation of forces and strains can also be expressed as in concrete

$$[N_c] = [D_c][\varepsilon_c] \quad (2.4)$$

where E_c and ν_c are respectively elastic modulus and Poisson's ratio of concrete,

$$[N_c] = \{N_x^c, N_y^c, \bar{N}_{xy}^c\}^T, \quad \bar{N}_{xy}^c = (N_{xy}^c + N_{yx}^c)/2,$$

$$[D_c] = \frac{E_c h}{1-\nu_c^2} \begin{bmatrix} 1-\rho_x & \nu_c(1-\rho_x) & 0 \\ \nu_c(1-\rho_y) & (1-\rho_y) & 0 \\ 0 & 0 & (1-\rho_{xy})(1-\nu_c)/2 \end{bmatrix}$$

In the case of the slide between steel and concrete is not caused in the process of reinforced concrete deformation, the force-strain relations of reinforced concrete can be written in the forms^[8]

$$[N]_s = ([D_c] + [D_s])[\varepsilon_s] \quad (2.5)$$

where $[N]_s = (N_x^s + N_x^c, N_y^s + N_y^c, \bar{N}_{xy}^s + \bar{N}_{xy}^c)$.

Herein, since the ratios of reinforcement are the function of x and y , every element in the relation matrix equation (2.5) is the function of x and y .

III. Computational Approach

Shell equations

In geometrically nonlinear analysis, both Updated Lagrangian and Total Lagrangian formulations are considered. The local Cartesian coordinate system is used for geometrical nonlinear formulations. The Green strain tensor can be expressed as

$$e_{ij} = (U_{i,j} + U_{j,i} + U_{k,i} \cdot U_{k,j}) / 2 \tag{3.1}$$

in which e_{ij} is nonlinear strain tensor, and U_i is displacement tensor.

An increment form of principle of virtual work, based on the Updated Lagrangian formulation, is as follows

$$\int \Delta_i S_{ij} \delta \Delta_i e_{ij} dV_i + \int \tau_{ij} \delta \Delta_i \eta_{ij} dV_i = \delta W - \int \tau_{ij} \delta \Delta_i e_{ij} dV_i \tag{3.2}$$

where δW is external incremental virtual work, the Green strain $\Delta_i e_{ij}$ and 2nd Piola-Kirchhoff stresses $\Delta_i S_{ij}$ are referred to the configuration at time t . The Cauchy stresses are represented as τ_{ij} . The incremental Green strains can be simply written as

$$\Delta_i e_{ij} = \Delta_i e_{ij} + \Delta_i \eta_{ij}, \quad \Delta_i e_{ij} = (\Delta_i U_{i,j} + \Delta_i U_{j,i}) / 2, \quad \Delta_i \eta_{ij} = (\Delta_i U_{k,i} \cdot U_{k,j}) / 2 \tag{3.3}$$

where $\Delta_i e_{ij}$ and $\Delta_i \eta_{ij}$ are the linear and quadratic parts of $\Delta_i e_{ij}$.

Shell elements

The elements for analysing shell structures have been reviewed in ref. [9]. In general, the use of curved shell finite elements will give a better geometrical representation, and the solution converges much faster than that using both simple flat shell elements^[10,11] and 3D isoparametric solid element^[12]. The use of a curved shell element, therefore, allows a relatively coarse mesh to be used to achieve a desired degree of accuracy. At the same time this reduces storage requirement for the solution.

herein, the Ahmad degenerated shell element (a nine-node isoparametric shell element)^[15] with Lagrangian interpolation functions for the displacement fields is adopted. Elastic stiffness, geometric stiffness, load vector due to initial stress, and the external load can be derived based on the following displacement fields once the geometry and the constitutive relationship are described over the element.

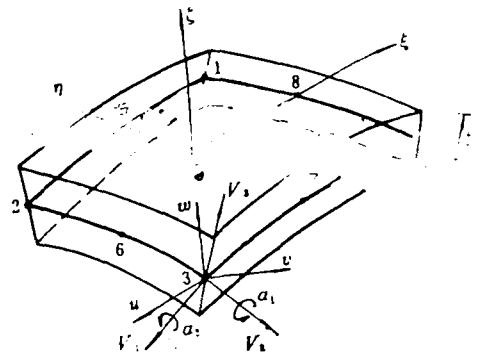


Fig. 1 Shell element configuration

$$U_i = \sum_{k=1}^n N^k(\xi, \eta) u_i^k + \frac{\xi}{2} \sum_{k=1}^n N^k(\xi, \eta) \cdot h^k (V_{1i}^k \alpha_1^k - V_{2i}^k \alpha_2^k) \tag{3.4}$$

where V_{1i}^k and V_{2i}^k are mutually orthogonal unit vectors which are contained in the plane normal to the V_{3i}^k direction which is constructed from the normal coordinate of the top and bottom surfaces at node i as shown in Fig. 1.

IV. Nonlinear Solution Procedures

In order to characterize overall behaviour of solution systems, the following non-dimensional scalar quantity is suggested

$$S_p = \frac{\dot{u}_0^T \bar{R}}{\dot{u}^T \bar{R}} = \left(\frac{\Delta p^t}{\Delta p^1} \right)^2 \frac{(\Delta u^1)^T K_i (\Delta u^1)}{(\Delta u^t)^T K_i (\Delta u^t)} \tag{4.1}$$

where S_p is denoted as 'current stiffness parameter'^[13]. A dot denotes differentiation with respect to the load parameter p . Index 0 indicates initial state. \bar{R} is a characterizing reference load which for instance may be chosen equal to $(\bar{p} \cdot R_{ref})$.

It is readily seen from equation (4.1) that current stiffness parameter has initial value of unity for any non-linear system. It is less than unity when the system becomes 'softer' than the initial system and greater than unity for stiffening systems.

In this way, we may divide load-displacement space into two kinds of type (see Fig 2) based on the parameter S_p . One is singular region with $|S_p| \leq S_{p,c} < 1$, in which the solution path is near limit point and the stiffness at some point is near singular. The other is nonsingular region with $|S_p| > S_{p,c}$, in which the nonlinear set of equations may be solved by using conventional methods, e.g. iterative method, step-by-step method, and their combination.

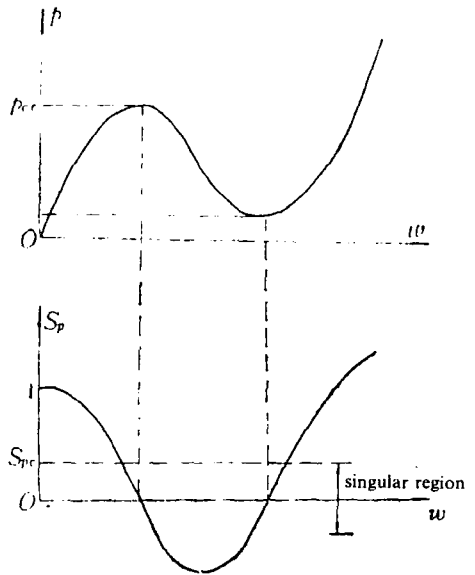


Fig. 2 Load-displacement space and current stiffness parameter

In singular region, we adopt a modified Newton-Raphson version of the Riks-Crisfield arc-length control algorithm^[14] to trace incrementally the load-displacement curve. Many experiences have shown RC arc-length procedure is very successful as a convenient means of statically traversing bifurcation points that arise in shell post-buckling analyses.

V. Nonlinear (Postbuckling) Numerical Analyses.

Nonlinear stability analysis of cylindrical shell

In order to prove the reliability and availability of the theory and method given in this paper, we analyse a cylindrical panel shell simply supported along its straight edges and free along the curved edge (see Fig. 3). The analysis results are well consistent with Sabir^[16] and Bergan^[13] (see Fig. 4).

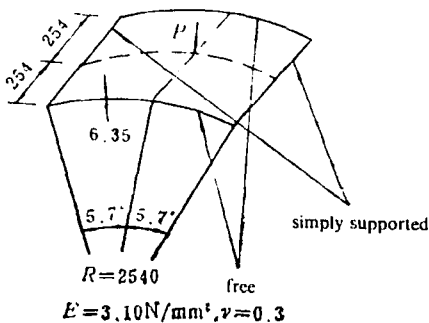


Fig. 3 The dimensions of cylindrical shell (unit, mm)

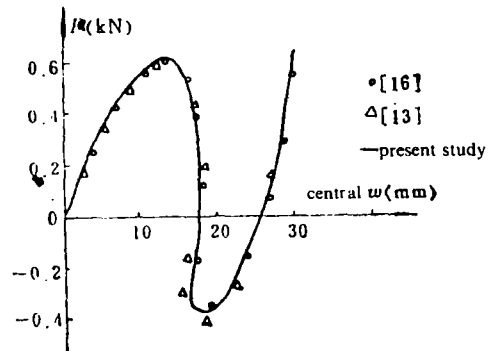


Fig. 4 The nonlinear analysis results of cylindrical shell

Nonlinear analysis of hyperbolic cooling tower shell

Fig. 5 presents a 90 (m) high reinforced concrete, its boundary conditions are free at top and discretely fixed at bottom, and under its own axisymmetric weight and unaxisymmetric wind load action. The nonlinear buckling of cooling tower which is made without and with one ring stiffened in throat, and the results are given in Fig. 6, in which the wind pressure data are given in table 1.

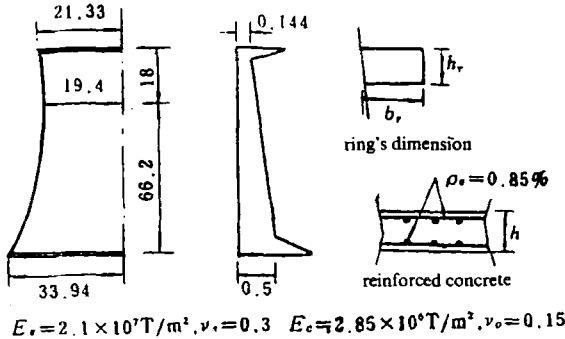


Fig. 5 The dimension of cooling tower (unit.m)

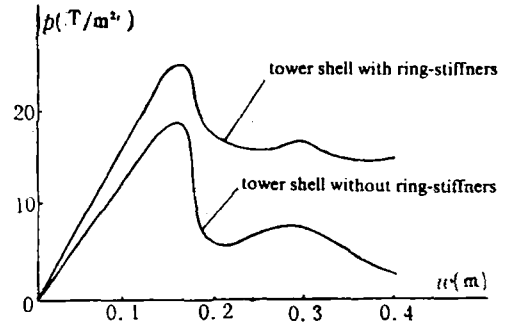


Fig. 6 The nonlinear buckling results of cooling tower (w is symmetric point on tower top against wind surface)

Table 1 The wind pressure data of cooling tower

$q = p \left[\frac{z + 72}{10} \right]^{2/7} \sum_{n=0}^{12} A_n \cos n\theta$			
$A_0 = 0.1167$	$A_1 = 0.2792$	$A_2 = 0.8198$	$A_3 = 0.5093$
$A_4 = 0.0917$	$A_5 = -0.1179$	$A_6 = -0.0933$	$A_7 = 0.0447$
$A_8 = 0.0083$	$A_9 = 0.0097$	$A_{10} = 0.0130$	$A_{11} = 0.0060$
$A_{12} = 0.0167$			

The results show, for the reinforced concrete hyperbolic cooling tower, the influence of geometric nonlinearities is very slight in pre-buckling, so that the results obtained from linear buckling analyses have good approximation. In addition, the instability critical load can be apparently raised by assembling the ring-stiffener. When the ring-stiffener whose dimension is $b_r = 0.5(m)$ and $h_r = 0.25(m)$ is assembled in the throat of cooling tower, the critical load can rise about 30%.

References

- [1] Mang, H.A., et al., Finite element instability analysis of hyperbolic cooling towers, *Advances in Civil Engineering Through Engineering Mechanics*, New York, ASCE (1977), 246 – 249.
- [2] Chan, A.S.L., et al., Cooling tower supporting columns and reinforced rings in small and large displacement analysis, *Comput. Meth. Appl. Mech. Engrg.*, **13** (1978), 1 – 26.
- [3] Abel, J.F., et al., Buckling of cooling towers, *J. Struct., Div.*, ASCE, **108** (1982), 2162 – 2174.
- [4] Abel, J.F., et al., Comparison of complete and simplified elastic buckling loads for cooling tower shells, IASS-RUB (1984), 309 – 318.
- [5] Mungan, I., et al., Nonlinear behaviour of cooling tower shells, IASS-RUB (1984), 298 – 307.
- [6] Mang, H.A., et al., Physically linear buckling analysis of reinforced concrete cooling towers—Design necessity or academic exercise?, IASS-RUB (1984), 279 – 297.
- [7] Dulacska, E., Buckling of reinforced concrete cooling tower shells, IASS-RUB (1984), 239 – 252.

- [8] Loo Wen-da and Li Long-yuan, Dynamic analyses of nonhomogeneous elastic hyperbolic cooling towers, *J. of Shanghai Mech.*, 2 (1987). (in Chinese)
- [9] Brebbia, C.A., *Finite Element Systems*. A handbook, A Comput. Mechanics Centre Publication (1982).
- [10] Thomas, G.R., et al., A triangular element based on generalized potential energy concepts, *Finite Elements for Thin Shells and Curved Members*, Chapter 9, Edited by D.G. Ashwell and R.H. Gallagher, Wiley (1976).
- [11] Dhatt, D.G., An efficient triangular shell element, *AIAA, J.*, **18** (1970).
- [12] Dovey, H.H., Extension of three-dimensional analysis to shell structures using the finite element idealization, Ph. D. Dissertation, Univ. of California, Berkeley, UC-SESM Report No. 74 - 2, Jan.(1974).
- [13] Bergan, P.G., et al., Solution techniques for nonlinear finite element problems, *Int. J. for Numerical Methods in Engrg.*, **12** (1978), 1677 – 1696.
- [14] Crisfield, M.A., A fast incremental/iterative solution procedure that handles snap-through, *Comput. and Struct.*, **13** (1983), 55 – 62.
- [15] Ahmad, S., et al., Analysis of thick and thin shell structures by curved finite elements, *Int. J. for Numerical Methods in Engrg.*, **2** (1970).
- [16] Sabir, and Lock. The application of finite elements to the large deflection geometrically nonlinear behaviour of cylindrical shells, *Variational Methods in Engineering*, ed. C.A. Brebbia and H. Tottenham, Southampton Univ. Press (1973), 7 – 67.